

# Insights into Poly(3-hexylthiophene)-*b*-Poly(ethylene oxide) Block Copolymer: Synthesis and Solvent-Induced Structure Formation in Thin Films

Hui Yang, Hao Xia, Guowei Wang, Juan Peng, Feng Qiu

State Key Laboratory of Molecular Engineering of Polymers, Department of Macromolecular Science, Fudan University, Shanghai 200433, China

Correspondence to: J. Peng (E-mail: juanpeng@fudan.edu.cn)

Received 21 June 2012; accepted 17 August 2012; published online 11 September 2012

DOI: 10.1002/pola.26353

**ABSTRACT:** We report the synthesis, characterization, and solvent-induced structure formation in thin films of an amphiphilic rod-coil conjugated block copolymer, poly(3-hexylthiophene)-*b*-poly(ethylene oxide). The diblock copolymers were prepared by a facile click reaction and their characterizations as well as thermal, crystalline, optical properties, and self-assembly behavior have been investigated in detail. A series of morphologies including two-phase separated nanostructure, nanofibrils, and their mixed morphology could be obtained depending on the selectivity of solvents to different

blocks. Structural analyses demonstrate there is a subtle balance between microphase separation of copolymer and the  $\pi$ - $\pi$  stacking of the conjugated P3HT and such balance can be controlled by changing the solvents of different selectivity in solution and the length of P3HT block. © 2012 Wiley Periodicals, Inc. *J Polym Sci Part A: Polym Chem* 50: 5060–5067, 2012

**KEYWORDS:** block copolymers; click reaction; conjugated polymers; rod-coil; self-assembly

**INTRODUCTION** Rod-coil block semiconducting copolymers have gained immense interest over the past few years because they combine the optical and electronic properties of conjugated polymers with the fascinating self-assembly properties of block copolymers.<sup>1</sup> In rod-coil block copolymers, flexible coil-like chains are covalently bonded to rod-like chains to tailor the structures of conjugated blocks and their self-assembly behaviors rely on four thermodynamic parameters: the Flory-Huggins strength of segregation ( $\chi N$ , where  $N$  is the molecular length), which parameterizes the interactions between chemically dissimilar blocks, the Maier-Saupe interaction relating the rod-rod alignment tendency ( $\mu N$ ), the volume fraction of coil ( $\phi_{\text{coil}}$ ) and the geometrical asymmetry of the system ( $\nu$ ).<sup>2</sup> These characteristics can give rise to unconventional phase-separated morphologies, which remain relatively unexplored and less understood than those obtained with classical coil-coil block copolymers.

Increasingly, solvent induced ordering has been used to tailor the nanodomain morphologies in block copolymers.<sup>3,4</sup> For a given copolymer system, a particular solvent may be classified as neutral or selective, according to whether it is (i) a good solvent for both blocks, or (ii) a good solvent for one but a poor or nonsolvent for the other.<sup>5</sup> In general, a neutral solvent distributes itself nearly equally between microdomains and can screen the unfavorable contact of

different blocks. By manipulating the solvent selectivity, the degree of microphase separation between blocks can be shifted. On one hand, the effects of solvent are focused on the block copolymer solution system where the selectivity drives micellization.<sup>6,7</sup> On the other hand, the effects of solvent are devoted to the block copolymer thin films by solvent annealing which usually leads to the formation of various metastable ordered structures.<sup>8,9</sup> By employing solvent effects to tailor the microphase separation of rod-coil, block copolymers can optimize the thin film morphology and offer the opportunity to improve their optoelectronic properties.

Among semiconducting polymers, regioregular poly(3-alkylthiophenes) (P3ATs) are one of the most promising conjugated polymers because of their good solubility, chemical stability, excellent electronic properties, as well as facile preparation.<sup>10</sup> These superior characteristics are readily accessible for optoelectronic device applications such as organic field-effect transistors,<sup>11</sup> photovoltaic cells,<sup>12,13</sup> and sensors.<sup>14</sup> Recently, many research groups synthesized P3AT-based rod-coil block copolymers, such as poly(3-hexylthiophene)-*b*-poly(vinylpyridine) (P3HT-*b*-PVP),<sup>15</sup> poly(3-hexylthiophene)-*b*-poly(methyl methacrylate) (P3HT-*b*-PMMA),<sup>16,17</sup> poly(3-hexylthiophene)-*b*-poly(lactide) (P3HT-*b*-PLA),<sup>18,19</sup> poly(3-alkylthiophene)-*b*-poly(ethylene oxide) (P3AT-*b*-PEO),<sup>20,21</sup> poly(3-hexylthiophene)-*b*-polystyrene (P3HT-*b*-PS),<sup>22,23</sup>

Additional Supporting Information may be found in the online version of this article.

© 2012 Wiley Periodicals, Inc.

and poly(3-alkylthiophene)-block-poly(arylisocyanide).<sup>24,25</sup> Such copolymers are usually prepared using a grafting-from approach, where an end-functionalized polythiophene is used as a macroinitiator for the polymerization of a second block, or a grafting-to approach allows each block to be prepared separately and then linked together. In recent years, “click” chemistry between azido and alkynyl groups has attracted increasing attention due to its high efficiency and, since 2008 this technique has been extended to preparation of block copolymers containing conjugated segments, such as P3HT-*b*-PS,<sup>26</sup> polythiophene-*b*-poly( $\gamma$ -benzyl L-glutamate) (P3HT-*b*-PBLG),<sup>27</sup> and poly(3-hexylthiophene)-*b*-poly(acrylic acid) (P3HT-*b*-PAA).<sup>28,29</sup> Very recently, diblock copolymer poly(3-hexylthiophene)-*b*-poly(ethylene oxide) (P3HT-*b*-PEO) was synthesized by click reaction from 2,5-dibromohexylthiophene monomer and they can form hierarchical assembly structures of isolated, bundled, and branched nanofibers in solutions<sup>30</sup> and exhibit simultaneous ionic and electronic conductivity when used in a battery cathode.<sup>31</sup>

In this article, we report the synthesis, characterization, and solvent-induced structure in thin films of an amphiphilic rod-coil block copolymer P3HT-*b*-PEO. The block copolymers were synthesized using a combination of modified Grignard metathesis polymerization (GRIM) and click reaction between ethynyl-terminated P3HT and azide-terminated PEO. The monomer used here was 2-bromo-5-iodo-3-hexylthiophene, which has good selectivity of activation by isopropylmagnesium chloride and hence ensure the narrow PDI and high regioregularity.<sup>32,33</sup> Their characterizations as well as thermal, crystalline, and optical properties have been investigated in detail. The solvent effects on the copolymer phase structures were explored. It revealed that there is a subtle balance between microphase separation of copolymer and the  $\pi$ - $\pi$  stacking fibrillar aggregates of the conjugated P3HT and such balance can be controlled by changing the solvents of different selectivity in solution.

## EXPERIMENTAL

### Materials

The monomer 2-bromo-5-iodo-3-hexylthiophene was synthesized according to the literature.<sup>34</sup> Copper(I) bromide (CuBr, 95%), Isopropylmagnesium chloride [*i*-PrMgCl, 2.0 M in tetrahydrofuran (THF)], ethynylmagnesium bromide (0.5 M in THF), 2-bromoisobutyl bromide, N, N, N', N'', N'''-pentamethyldiethylenetriamine (PMDETA), (1,3-bis(diphenylphosphino)-propane)-dichloronickel(II) (Ni(dppp)Cl<sub>2</sub>) and methoxyl poly(ethylene oxide) (PEO) were purchased from Aldrich and used as received. The other reagents and solvents were purchased from Sinopharm Chemical Reagent (SRC). THF and dichloromethane (CH<sub>2</sub>Cl<sub>2</sub>) were freshly dried over sodium benzophenone ketyl and calcium hydroxide respectively. All other solvents were used as received.

### Synthesis of Ethynyl-Terminated Poly(3-hexylthiophene) (P3HT-C≡CH)

The typical synthesis procedure of the P3HT-C≡CH ( $M_n = 8000$  g/mol, PDI = 1.1) was as follows. Into an oven-dried

round-bottom flask with side tubes was added 3.73 g (10 mmol) of 2-bromo-5-iodo-3-hexylthiophene monomer under N<sub>2</sub> and then evacuated under reduced pressure to remove water and oxygen inside. After adding dry THF (100 mL) with a syringe, the solution was stirred at 0 °C under N<sub>2</sub>. Isopropylmagnesium chloride in THF (5 mL, 10 mmol) was added and allowed to react for 30 min at 0 °C. Subsequently, The solution was heated up to 35 °C followed by the addition of Ni(dppp)Cl<sub>2</sub> catalyst (108.4 mg, 0.2 mmol). The resulting mixture was stirred for 10 min, producing intermediate P3HT, which was then reacted with 0.5 M ethynylmagnesium bromide (10 mL, 5 mmol) for an additional 5 min at room temperature. After the reaction was quenched in methanol and a dark-purple solid was obtained, the product was then isolated via filtration, washed with excess methanol and hexane, and dried under vacuum to yield 1.0 g of P3HT-C≡CH (60% yield). The P3HT-C≡CH with other molecular weights was synthesized in the same way. GPC:  $M_n = 8000$  g/mol, PDI = 1.1. <sup>1</sup>H NMR (500 MHz, CDCl<sub>3</sub>,  $\delta$ ): 6.98 (s), 3.52 (s), 2.8 (t), 1.71 (m), 1.44 (m), 1.35 (m), 0.92 (t).

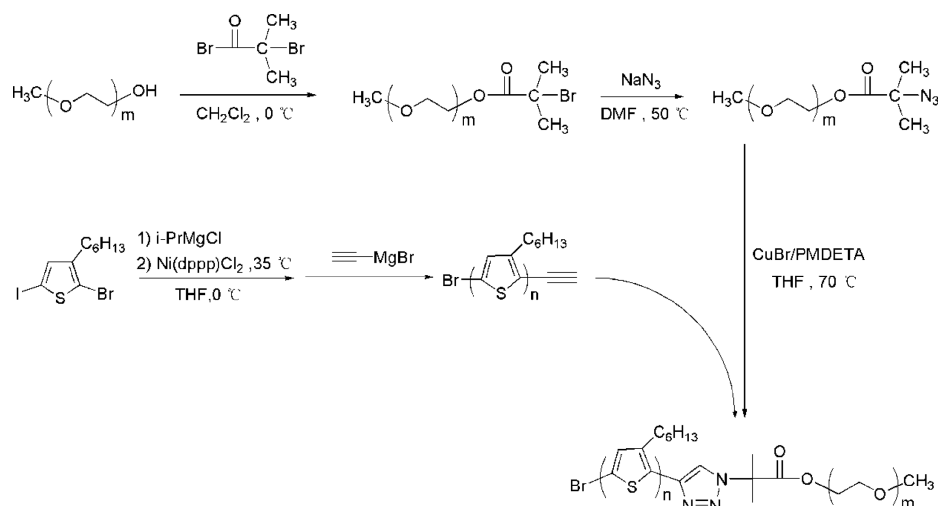
### Synthesis of Azide-Terminated Methoxyl Poly(ethylene oxide) (PEO-N<sub>3</sub>)

The typical preparation procedure for bromo-terminated methoxyl poly(ethylene oxide) (PEO-Br): Dried PEO (15.0 g, 3 mmol) and triethylamine (4.3 mL, 30 mmol) were dissolved in anhydrous dichloromethane (150 mL). 2-Bromoisobutyl bromide (3.7 mL, 30 mmol) was added dropwise at 0 °C in 1 h and the mixture was stirred for another 24 h at room temperature. After filtering the precipitated salt, the crude product was washed with distilled water three times. The organic layer was dried with anhydrous magnesium sulfate (MgSO<sub>4</sub>), concentrated, and then precipitated into cold diethyl ether. The polymer was dried for 24 h in a vacuum oven at room temperature and 13.7 g white solid was obtained in 91% yield. GPC:  $M_n = 6400$  g/mol, PDI = 1.01, <sup>1</sup>H NMR (500 MHz, CDCl<sub>3</sub>,  $\delta$  ppm): 3.37–3.82 (m), 2.07 (s).

The typical preparation procedure for azide end-functionalized poly(ethylene oxide) (PEO-N<sub>3</sub>): The obtained PEO-Br (10.0 g, 2 mmol) was dissolved in DMF (100 mL), and sodium azide (1.3 g, 20 mmol) was added to the solution. The mixture was stirred for 24 h at 50 °C. After filtering the precipitated salt, the solvent was removed in vacuum. Subsequently, the crude product was redissolved in dichloromethane and washed three times with distilled water. The organic layer was dried with anhydrous magnesium sulfate, concentrated, and then precipitated in cold diethyl ether. The polymer was dried for 24 h in a vacuum oven at room temperature and 8.4 g white solid was obtained in 84% yield. GPC:  $M_n = 6400$  g/mol, PDI = 1.01, <sup>1</sup>H NMR (500 MHz, CDCl<sub>3</sub>,  $\delta$  ppm): 3.82–3.37 (m), 1.88 (s).

### Synthesis of Poly(3-hexylthiophene)-*b*-poly(ethylene oxide)

The typical synthesis procedure of the P3HT-*b*-PEO ( $M_n = 14400$ , PDI = 1.18) was as follows. Into a 100 mL Schlenk flask, P3HT-C≡CH ( $M_n = 8000$  g/mol, 1.0 g, 0.125 mmol), PEO-N<sub>3</sub> (1.9 g, 0.375 mmol), CuBr (0.1 g, 0.7 mmol),



**SCHEME 1** Synthesis route of P3HT-*b*-PEO block copolymer.

PMDETA (0.15 mL, 0.7 mmol), and dry THF (40 mL) were added. The reaction mixture was degassed by three freeze-pump-thaw cycles in liquid N<sub>2</sub>, and then stirred at 70 °C for 24 h. After removing THF by rotary evaporation, the crude product was redissolved in methanol and purified by an ultrafiltration membrane to remove copper catalyst residues and the excess PEO-N<sub>3</sub>. Finally, dark purple solid was obtained after removing methanol. The P3HT-*b*-PEO with other molecular weights was synthesized in the same way. GPC:  $M_n = 14400$  g/mol, PDI = 1.18. <sup>1</sup>H NMR (500 MHz, CDCl<sub>3</sub>,  $\delta$  ppm): 7.78 (s), 6.98 (s), 4.33 (t), 3.78 (m), 3.64 (m), 3.60 (s), 3.5 (t), 3.38 (s), 2.8 (t), 2.57 (m), 2.01 (s), 1.70 (m), 1.43 (m), 1.36 (m), 0.92 (t).

### Characterization

Gel permeation chromatography (GPC) was operated at 35 °C using an Agilent 1100 system equipped with both G1362A refractive-index and G1314A UV detectors (eluent: THF; calibration: polystyrene standards). <sup>1</sup>H NMR spectra were recorded on a DMX500 MHz spectrometer in CDCl<sub>3</sub> and D<sub>2</sub>O with tetramethylsilane as the internal standard. Fourier transform infrared (FTIR) spectra were obtained at a Magna-550 FT-IR spectrometer (NaCl tablet). Differential scanning calorimetry (DSC) thermograms and thermogravimetric (TGA) analysis were measured using TA DSC Q2000 at a heating rate of 10 °C/min under N<sub>2</sub> flow and TA TGA Q5000, respectively. X-ray diffraction (XRD) was performed on a PANalytical X'Pert PRO X-ray diffractometer using Cu K $\alpha$  radiation ( $\lambda = 1.541$  Å) operating at 40 kV and 40 mA. UV-vis absorption spectra were recorded on Perkin Elmer Lambda 35 UV-vis spectrophotometers. Atomic force microscopy (AFM) was carried out on a Veeco Multimode AFM Nanoscope IV in tapping mode. Transmission electron microscope (TEM) imaging was performed on a Tecnai G<sup>2</sup> 20-Twin transmission electron microscope operated at 200 kV. The ultra filtration membrane separator was purchased from Shanghai Institute of Applied Physics, Chinese Academy of Science, the cut-off molecular weight of used poly(ether

sulfone) film:  $M_w$  (cut-off) = 20000 g/mol (calibrated by globin).

### Film Preparation

Thin films for AFM were prepared by spin-coating 0.5 mg/mL copolymer solutions in different solvents on silicon wafers at 3000 r/min for 60 s. The samples for XRD measurements were prepared by drop-casting 10 mg/mL copolymer toluene solutions onto silicon wafers. As for TEM analysis, the samples were prepared by drop-casting 0.5 mg/mL copolymer solutions in anisole on copper grids, followed by evaporation of the solvent at ambient. The silicon wafers were pre-cleaned in a piranha solution (70/30 v/v of 98% H<sub>2</sub>SO<sub>4</sub>/30% H<sub>2</sub>O<sub>2</sub>) overnight and then thoroughly washed with deionized water and blown dry with nitrogen.

## RESULTS AND DISCUSSION

### Synthesis and Characterization of P3HT-*b*-PEO Diblock Copolymer

The straight-forward synthetic route to copolymer P3HT-*b*-PEO is depicted in Scheme 1. The synthesis started from 2-bromo-5-iodo-3-hexylthiophene and compared with the 2,5-dibromohexylthiophene, the monomer used here has better selectivity of activation by isopropylmagnesium chloride and hence ensure P3ATs with targeted molecular weights, narrow PDI, and high regioregularity. Ethynyl-terminated P3HT (P3HT-C≡CH) was successfully obtained upon quenching the polymerization by ethynylmagnesium bromide. It is worth noting that P3HT-C≡CH was highly sensitive to the isolation and purification conditions employed. Since coupling by-product may be obtained after subjecting the polymer to sequential Soxhlet extraction, purification at room temperature is necessary to get monomodal GPC result. The incorporation of ethynyl terminal group was identified by <sup>1</sup>H NMR spectrum. As shown in Figure 1, a resonance singlet signal appeared at 3.52 ppm, which is attributed to the proton in the ethynyl group.

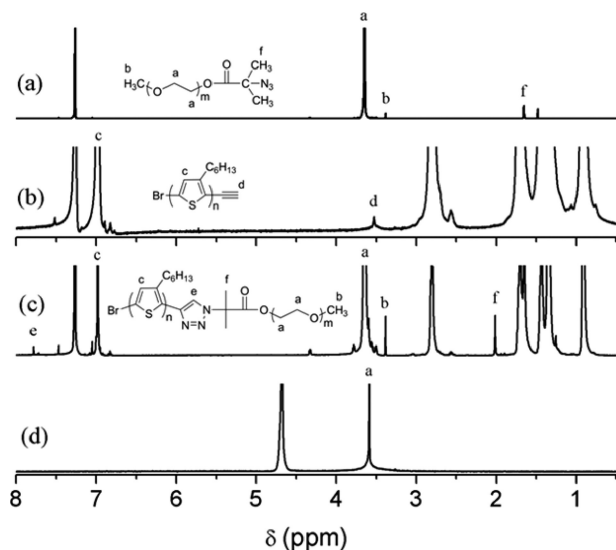


**FIGURE 1**  $^1\text{H}$  NMR spectra of (a)  $\text{PEO-N}_3$ , (b)  $\text{P3HT-C}\equiv\text{CH}$ , (c)  $\text{P3HT-}b\text{-PEO}$  in  $\text{CDCl}_3$ , and (d)  $\text{P3HT-}b\text{-PEO}$  in  $\text{D}_2\text{O}$ .

The other block, azide end-capped PEO ( $\text{PEO-N}_3$ ), was synthesized by esterification of the hydroxyl end group by 2-bromoisobutyryl bromide, and sequentially the bromide was converted to azide by reaction with  $\text{NaN}_3$ . The successful functionalization of PEO with azide group was proved by FTIR spectra of  $\text{PEO-Br}$  and  $\text{PEO-N}_3$ . As shown in Figure 2, the absorption band at  $1740\text{ cm}^{-1}$  indicates the ester bond stretching while the peak at  $2110\text{ cm}^{-1}$  demonstrates the azide stretching, suggesting the introduction of azide group into the PEO.

Finally, the two building blocks were connected by “click” the azido and ethynyl groups in the presence of  $\text{CuBr}/\text{PMDETA}$  in THF at  $70\text{ }^\circ\text{C}$  for 24 h. An ultrafiltration through a membrane with a certain molecular weight cutoff can eas-

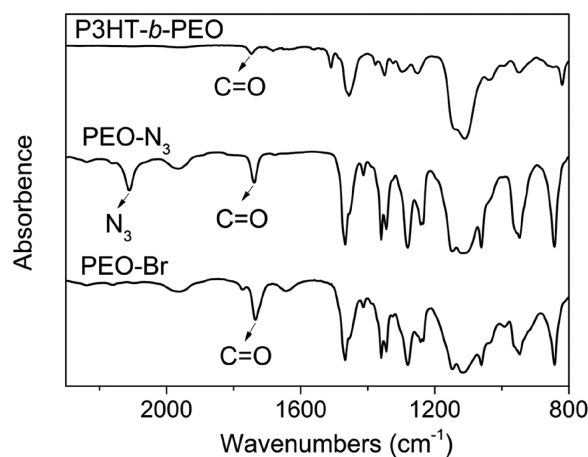


**FIGURE 2** FTIR spectra of bromide-terminated PEO, azide-terminated PEO, and  $\text{P3HT-}b\text{-PEO}$ . The signals at  $1740$  and  $2110\text{ cm}^{-1}$  were assigned to the carbonyl and azide stretching frequency respectively.

**TABLE 1** Summary of Compositions and Molecular Weights of  $\text{P3HT-}b\text{-PEO}$  Block Copolymers

Polymer	$M_n$ , P3HT (g/mol)	$M_n$ , PEO (g/mol)	$M_n$ , total (g/mol)	PDI
$\text{P3HT-}b\text{-PEO-1}$	8000	6400	14,400	1.18
$\text{P3HT-}b\text{-PEO-2}$	10,700	6400	17,700	1.17
$\text{P3HT-}b\text{-PEO-3}$	20,500	6400	25,000	1.36

ily remove the excess  $\text{PEO-N}_3$  which was initially fed for consuming all the  $\text{P3HT-C}\equiv\text{CH}$ . Consequently, pure and clean  $\text{P3HT-}b\text{-PEO}$  block copolymer was produced and its chemical structure was characterized by  $^1\text{H}$  NMR and FTIR spectroscopy. As shown in Figures 1 and 2, the appearance of the triazole ring signal ( $\delta = 7.78\text{ ppm}$ ) as well as the disappearance of ethynyl signal ( $\delta = 3.52\text{ ppm}$ ) and  $\nu_{\text{N}_3}$  IR signal ( $2110\text{ cm}^{-1}$ ) indicate the successful synthesis of  $\text{P3HT-}b\text{-PEO}$ . The resulting  $\text{P3HT-}b\text{-PEO}$  block copolymers are summarized in Table 1. The molecular weight of P3HT block is varied from  $8000\text{ g/mol}$  to  $20,500\text{ g/mol}$  with the fixed molecular weight of PEO block.

Interestingly, the  $\text{P3HT-}b\text{-PEO}$  in different deuterated solvents exhibit different  $^1\text{H}$  NMR spectra. The  $^1\text{H}$  NMR spectrum of  $\text{P3HT-}b\text{-PEO}$  in  $\text{CDCl}_3$  displays all the proton resonance. However, in  $\text{D}_2\text{O}$  which is a good solvent for PEO but a poor solvent for P3HT, all the signals attributed to the protons in the P3HT block disappear while only a singlet peak at  $\delta = 3.59\text{ ppm}$  attributed to the methylene group in PEO can be observed. This indicates that the PEO blocks are in an extended solvated state in  $\text{D}_2\text{O}$  and form a shield around the P3HT aggregates.

Figure 3 displays the representative GPC profiles of  $\text{P3HT-C}\equiv\text{CH}$ ,  $\text{PEO-N}_3$ , crude  $\text{P3HT-}b\text{-PEO}$  and isolated pure  $\text{P3HT-}b\text{-PEO}$  after removal of excess  $\text{PEO-N}_3$ . It can be found that the GPC curve of  $\text{P3HT-C}\equiv\text{CH}$  exhibit a monomodal peak with the molecular weight of  $8000\text{ g/mol}$  and PDI of 1.1. Upon attaching  $\text{PEO-N}_3$ , the crude product exhibited

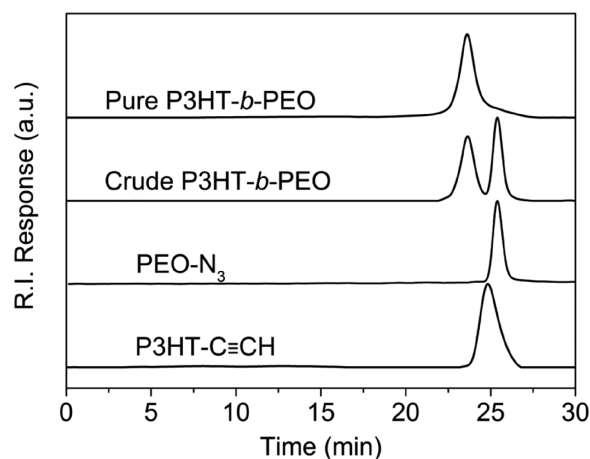


**FIGURE 3** GPC traces of  $\text{P3HT-C}\equiv\text{CH}$ ,  $\text{PEO-N}_3$ , their coupling crude product, and isolated  $\text{P3HT-}b\text{-PEO}$ .

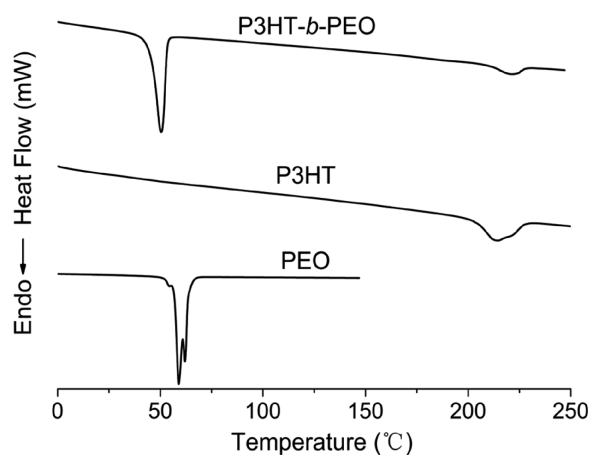


FIGURE 4 DSC endotherms of PEO, P3HT, and P3HT-*b*-PEO.

two peaks corresponding the target diblock polymer and excess PEO-N<sub>3</sub>. After removing excess PEO-N<sub>3</sub> via an ultrafiltration membrane, the pure diblock polymer shows a higher molecular weight of 14400 g/mol with the maintenance of low PDI of 1.18. In the following, the P3HT-*b*-PEO represented P3HT-*b*-PEO-1 ( $M_n = 14400$  g/mol, PDI = 1.18) as a model copolymer for detailed investigation if without specification.

#### Thermal and Crystalline Behaviors

To investigate the thermal properties of the P3HT-*b*-PEO diblock copolymer, DSC (Fig. 4) and TGA (Fig. 5) measurements were performed. As shown in Figure 4, DSC measurements of the P3HT-*b*-PEO block copolymer show the melting temperature ( $T_m$ ) for P3HT and PEO blocks at 221 and 51 °C, respectively. The two melting points in copolymer system indicate that P3HT and PEO crystallize independently to form their own crystalline domain with microphase separation. The cooling thermograms with two-crystallization peak in P3HT-*b*-PEO also prove microphase separation during the DSC cooling process (Supporting Information Fig. S1). Compared with the  $T_m$  of pure P3HT and PEO homopolymers at 214 and 58 °C, respectively, the  $T_m$  of P3HT block increases

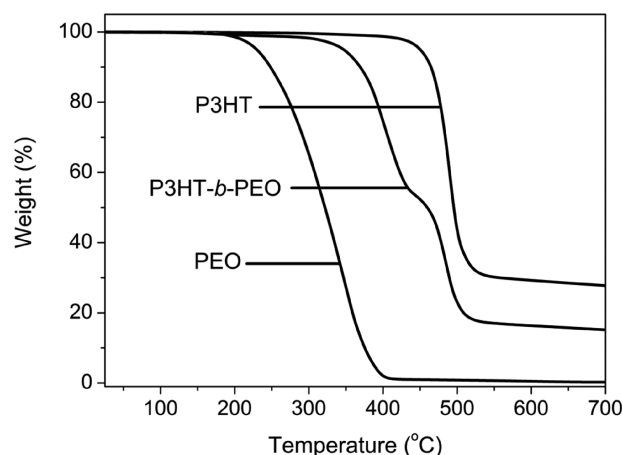


FIGURE 5 TGA curves of PEO, P3HT, and P3HT-*b*-PEO.

because the covalently bonded movable PEO block hampers the mobility of P3HT. Therefore, it needs higher temperature to change from crystalline state to melted state. The  $T_m$  of PEO block decreases due to the P3HT block disturbing the organization of the PEO into highly crystalline domains. The similar hinderance effect of the P3HT segment on the efficient crystallization of polyethylene (PE) was reported by Janssen et al.<sup>35</sup>

Figure 5 shows the TGA curve of P3HT, PEO, and P3HT-*b*-PEO. In nitrogen atmosphere, a two-stage weight loss behavior is observed in P3HT-*b*-PEO system from 362 to 465 °C and above 465 °C. The first one is due to the degradation of PEO segments. Compared with the TGA curve of PEO, it can be found that the incorporation of a rigid P3HT block into PEO has dramatically increased the degradation onset of PEO from 231 to 362 °C. The second degradation starts over 465 °C, which is attributed to the cleavage of alkyl side chains of P3HT. Over 700 °C, a remaining 16% undecomposed compound in N<sub>2</sub> can be attributed to the P3HT backbone.

The crystalline structures of the P3HT homopolymer and P3HT-*b*-PEO copolymer are characterized using XRD, which show a recognizable diffraction peak at  $2\theta = 5.8^\circ$  assigned to the (100) reflection of the P3HT chains due to the inter-layer side chain spacing of 15.2 Å in both systems (Fig. 6). The XRD data suggest the P3HT crystalline planes are mainly oriented normal to the films<sup>36</sup> and the introduction of PEO block has little impact on the arrangement of P3HT block.

#### Optical Properties

The photophysical properties of the P3HT-*b*-PEO copolymer in both solution and film systems were investigated by UV-vis spectroscopy. Due to the amphiphilic nature of the copolymer, it is soluble in a wide range of solvents, including good solvents for both blocks, such as THF, or marginal solvents for P3HT, such as anisol, or PEO-selective solvents, such as ethyl acetate. However, the solutions of the copolymer in different type of solvents display different colors, typically, orange in good solvents for P3HT, and purple in poor

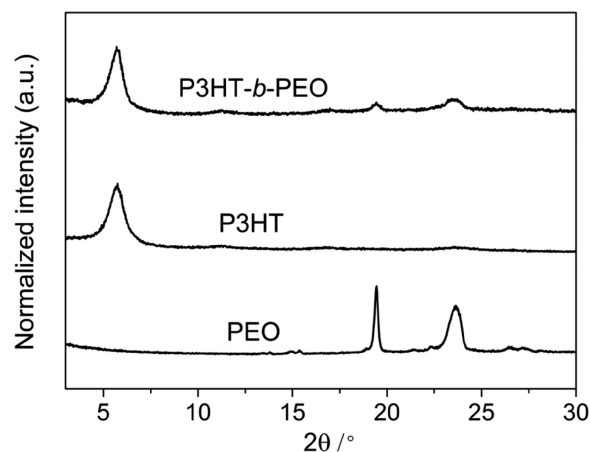


FIGURE 6 XRD profiles of PEO, P3HT, and P3HT-*b*-PEO casted from 10 mg/mL toluene solution.



**FIGURE 7** Color changes of P3HT-*b*-PEO (0.5 mg/mL) in different solvents, that is, THF, toluene, CHCl<sub>3</sub>, anisol, ethyl acetate, MeOH, and H<sub>2</sub>O (from left to right).

solvents for P3HT (Fig. 7). Such different color of the block copolymer solutions are related to their different absorption spectra and the optical properties of P3HT are influenced by the intrachain and interchain interactions of the materials. The UV-vis spectra of P3HT-*b*-PEO copolymer in three typical solvents were investigated [Fig. 8(a)]. It is shown that in THF, a single peak with a maximum at 450 nm was observed which is due to the  $\pi$ - $\pi^*$  transition of the polythiophene main chain. While in ethyl acetate, a bathochromic shift of the absorption spectrum was observed with the main peak at 510 nm and two vibronic peaks at 545 and 598 nm, respectively, which were attributed to the absorption of the strong interchain  $\pi$ - $\pi$  interaction. The bathochromic shift of the absorption peak in poor solvent for P3HT was also observed by Kamps et al.<sup>30</sup> In anisol, a marginal solvent for P3HT, the UV-vis spectra located in the middle with the main peak at 474 nm. The corresponding UV-vis spectra of P3HT-*b*-PEO thin films casted from different solvents were also recorded [Fig. 8(b)]. Compared with the absorption spectra in solutions, the absorption spectra of all the thin films exhibit bathochromically shifted absorption maxima with the main peak at 519 nm and two vibronic peaks at 553 and 603 nm, respectively.

#### Solvent-Induced Structure Formation in Thin Films

It is known that P3HT exist in two distinct conformations, that is, a random coil conformation and a planarized conformation depending on the temperature, concentration or quality of the solvents used.<sup>37</sup> The used solvents strongly influence the as-cast thin film morphology of copolymer on Si/SiO<sub>2</sub> substrates (Fig. 9). In THF which is a good solvent for both P3HT and PEO blocks, P3HT-*b*-PEO forms a two-phase separated nanostructure characteristic of block copolymers, which is due to the immiscibility of P3HT and PEO segments [Fig. 9(a)]. In marginal solvent, anisol for P3HT [Fig. 9(b)], a mixed morphology with both phase separated structure and much longer fibrillar structure are observed with the width and height of  $\sim$ 35 and 7 nm. Such fibrillar morphology originates from the  $\pi$ - $\pi$  interactions between the P3HT segments with a planarized conformation. Whereas in poor solvent for P3HT but selective for PEO (ethyl acetate),

only fibrillar structure is observed [Fig. 9(c)]. The morphological differences in different solvents are determined to a large extent by the competition between the microphase separation of copolymer and the  $\pi$ - $\pi$  stacking of the conjugated P3HT which dominates. In good solvent for both blocks, the copolymer is molecularly dissolved and microphase separation between P3HT and PEO dominates, leading to a two-phase separated nanostructure. Whereas in poor solvent for

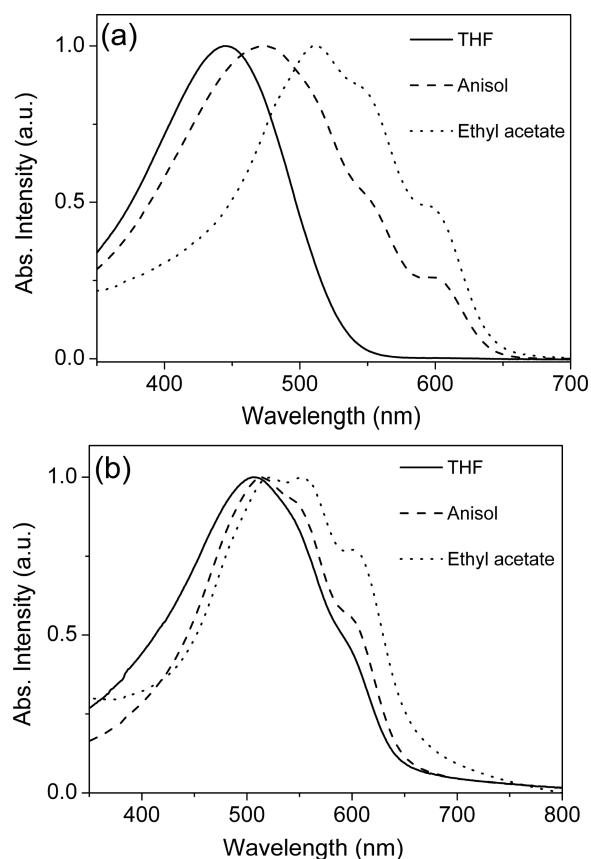


**FIGURE 8** UV-vis spectra of P3HT-*b*-PEO (a) in the different solvents and (b) in the thin films drop-cast from different solvents.

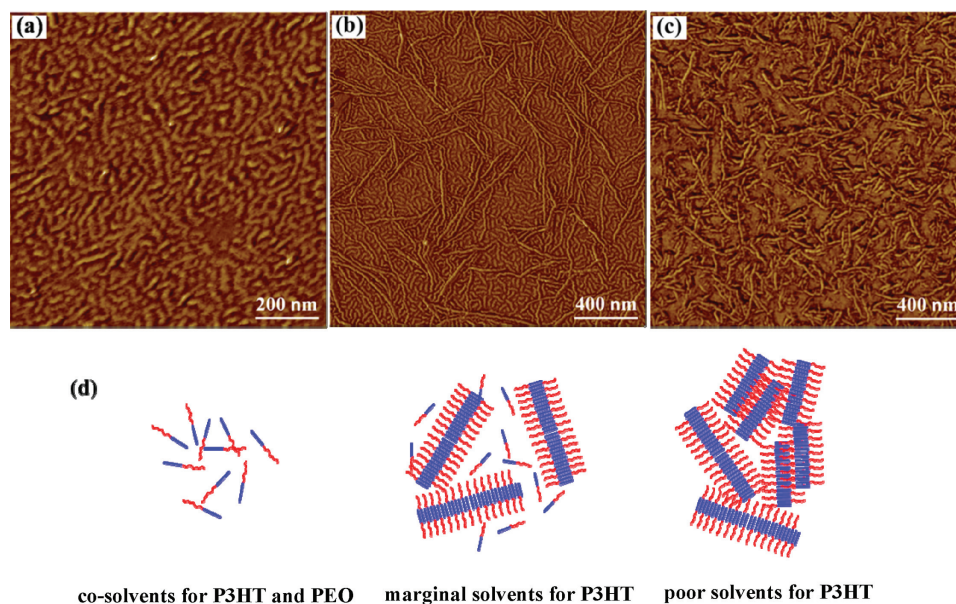


**FIGURE 9** AFM phase images of P3HT-*b*-PEO-1 thin films spin-coated from different solvents: (a) THF, (b) anisole, and (c) ethyl acetate. (d) Schematic representation of the P3HT-*b*-PEO-1 chains in different solvents.

P3HT, the  $\pi$ - $\pi$  interactions between the P3HT segments are stronger, resulting in the fibrillar morphology. In marginal solvent for P3HT, a coexistence of both phase-separated structure and fibrillar structure is observed. The possible structures of the copolymer chains in different solvents are schematically shown in Figure 9(d). It revealed that there is a subtle balance between microphase separation of copolymer and the  $\pi$ - $\pi$  stacking of the conjugated P3HT and such balance can be controlled by changing the solvents of different selectivity. Such structural variations are concomitant with the aforementioned distinctive solvatochromic changes in the photophysical properties.

In addition to the solvent, the length of P3HT block also influences the self-assembly behavior of copolymer. Three P3HT-*b*-PEO copolymers with the same length of PEO block and various lengths of P3HT block were dissolved in anisole to investigate their self-assembly behavior. As shown in

Figure 10(a), both phase separated structure and fibrillar structure are observed in P3HT-*b*-PEO-1 system. The consistent morphology measured by TEM [Fig. 10(a)] and AFM [Fig. 9(b)] indicated the dry AFM sample represented the case in the solution. With the increased length of P3HT block, fibrillar morphology with less phase-separated structure is observed in P3HT-*b*-PEO-2 system [Fig. 10(b)] and only fibrillar morphology without phase-separated structure is observed in P3HT-*b*-PEO-3 system [Fig. 10(c)]. Obviously, the  $\pi$ - $\pi$  stacking of P3HT with larger molecular weight is stronger compared with that of P3HT with lower molecular weight. Therefore,  $\pi$ - $\pi$  stacking of the conjugated P3HT dominates in P3HT-*b*-PEO-2 and 3 systems. The above results indicate the subtle balance between microphase separation of copolymer and the  $\pi$ - $\pi$  stacking of the conjugated P3HT can be well controlled by changing the solvents of different selectivity in solution and the length of P3HT block.

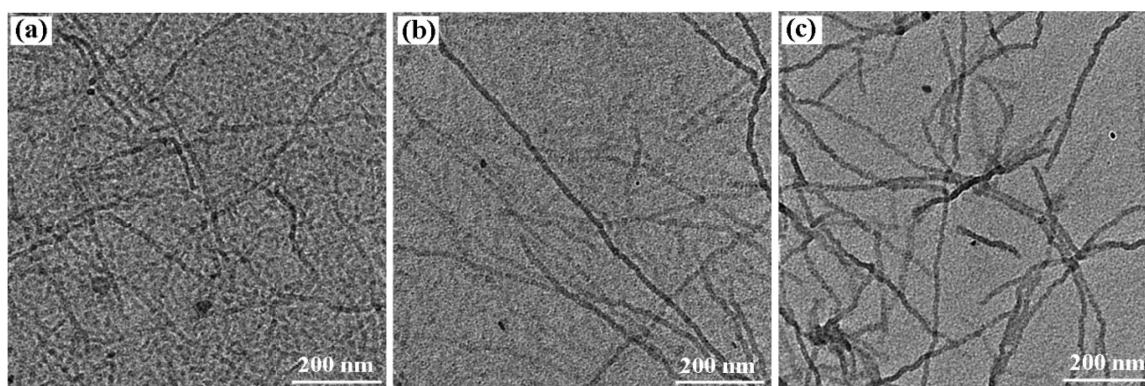


**FIGURE 10** TEM images of (a) P3HT-*b*-PEO-1, (b) P3HT-*b*-PEO-2, and (c) P3HT-*b*-PEO-3 in anisole with the concentration of 0.5 mg/mL.

## CONCLUSIONS

In summary, the amphiphilic rod-coil conjugated P3HT-*b*-PEO block copolymers with narrow PDI were successfully synthesized by a facile click reaction which coupling ethynyl-terminated poly(3-hexylthiophene) and azide-terminated poly(ethylene oxide). The synthesis started from 2-bromo-5-iodo-3-hexylthiophene, which has good selectivity of activation in GRIM method and hence ensure the narrow PDI and high regioregularity. Their characterizations as well as thermal, crystalline, optical properties, and self-assembly behavior have been investigated in detail using NMR, GPC, FT-IR, DSC, TGA, XRD, AFM, and TEM. A series of morphologies including two-phase separated nanostructure, nanofibrils and their mixed nanostructures could be obtained on films spin-coated from different solvents. The morphological differences arise from the subtle balance between microphase separation of copolymer and the  $\pi$ - $\pi$  stacking of the conjugated P3HT and such balance can be controlled by changing the solvents of different selectivity in solution and the length of P3HT block.

## ACKNOWLEDGMENTS

This work was financially supported by the National Natural Science Foundation of China (Grant No. 21074026 and 20990231) and National Basic Research Program of China (2011CB605700).

## REFERENCES AND NOTES

- Liu, C. L.; Lin, C. H.; Kuo, C. C.; Lin, S. T.; Chen, W. C. *Prog. Polym. Sci.* **2011**, *36*, 603–637.
- Tao, Y. F.; McCulloch, B.; Kim, S.; Segalman, R. A. *Soft Matter* **2009**, *5*, 4219–4230.
- Park, S.; Wang, J. Y.; Kim, B.; Chen, W.; Russell, T. P. *Macromolecules* **2007**, *40*, 9059–9063.
- Patra, S. K.; Ahmed, R.; Whittell, G. R.; Lunn, D. J.; Dunphy, E. L.; Winnik, M. A.; Manners, I. *J. Am. Chem. Soc.* **2011**, *133*, 8842–8845.
- Peng, J.; Han, Y. C.; Knoll, W.; Kim, D. H. *Macromol. Rapid Commun.* **2007**, *28*, 1422–1428.
- Craley, C. R.; Zhang, R.; Kowalewski, T.; McCullough, R. D.; Stefan, M. C. *Macromol. Rapid Commun.* **2009**, *30*, 11–16.
- He, M.; Zhao, L.; Wang, J.; Han, W.; Yang, Y. L.; Qiu, F.; Lin, Z. Q. *ACS Nano* **2010**, *4*, 3241–3247.
- Huang, W. H.; Chen, P. Y.; Tung, S. H. *Macromolecules* **2012**, *45*, 1562–1569.
- Yu, X. H.; Yang, H.; Wu, S. P.; Geng, Y. H.; Han, Y. C. *Macromolecules* **2012**, *45*, 266–274.
- Osaka, I.; McCullough, R. D. *Acc. Chem. Res.* **2008**, *41*, 1202–1214.
- Aiyar, A. R.; Hong, J. I.; Nambiar, R.; Collard, D. M.; Reichmanis, E. *Adv. Funct. Mater.* **2011**, *21*, 2652–2659.
- Thompson, B. C.; Kim, B. J.; Kavulak, D. F.; Sivula, K.; Mauldin, C.; Frechet, J. M. *J. Macromolecules* **2007**, *40*, 7425–7428.
- He, M.; Han, W.; Ge, J.; Yu, W. J.; Yang, Y. L.; Qiu, F.; Lin, Z. Q. *Nanoscale* **2011**, *3*, 3159–3163.
- Shiraki, T.; Dawn, A.; Tsuchiya, Y.; Shinkai, S. *J. Am. Chem. Soc.* **2010**, *132*, 13928–13935.
- Dai, C. A.; Yen, W. C.; Lee, Y. H.; Ho, C. C.; Su, W. F. *J. Am. Chem. Soc.* **2007**, *129*, 11036–11038.
- Lee, Y. J.; Kim, S. H.; Yang, H.; Jang, M.; Hwang, S. S.; Lee, H. S.; Baek, K. Y. *J. Phys. Chem. C* **2011**, *115*, 4228–4234.
- Moon, H. C.; Anthonysamy, A.; Kim, J. K.; Hirao, A. *Macromolecules* **2011**, *44*, 1894–1899.
- Boudouris, B. W.; Frisbie, C. D.; Hillmyer, M. A. *Macromolecules* **2008**, *41*, 67–75.
- Ho, V.; Boudouris, B. W.; McCulloch, B. L.; Shuttle, C. G.; Burkhardt, M.; Chabiny, M. L.; Segalman, R. A. *J. Am. Chem. Soc.* **2011**, *133*, 9270–9273.
- Park, S. J.; Kang, S. G.; Fryd, M.; Saven, J. G. *J. Am. Chem. Soc.* **2010**, *132*, 9931–9933.
- Gu, Z. J.; Kanto, T.; Tsuchiya, K.; Shimomura, T.; Ogino, K. *J. Polym. Sci. Part A: Polym. Chem.* **2011**, *49*, 2645–1652.
- Kaul, E.; Senkovskyy, V.; Tkachov, R.; Bocharova, V.; Komber, H.; Stamm, M.; Kiriy, A. *Macromolecules* **2010**, *43*, 77–81.
- Urien, M.; Erothu, H.; Cloutet, E.; Hiorns, R. C.; Vignau, L.; Cramail, H. *Macromolecules* **2008**, *41*, 7033–7040.
- Wu, Z. Q.; Ono, R. J.; Chen, Z.; Bielawski, C. W. *J. Am. Chem. Soc.* **2010**, *132*, 14000–14001.
- Wu, Z. Q.; Radcliffe, J. D.; Ono, R. J.; Chen, Z.; Li, Z. C.; Bielawski, C. W. *Polym. Chem.* **2012**, *3*, 874–881.
- Urien, M.; Erothu, H.; Cloutet, E.; Hiorns, R. C.; Vignau, L.; Cramail, H. *Macromolecules* **2008**, *41*, 7033–7040.
- Wu, Z. Q.; Ono, R. J.; Chen, Z.; Li, Z. C.; Bielawski, C. W. *Polym. Chem.* **2011**, *2*, 300–302.
- Pang, X. C.; Zhao, L.; Feng, C. W.; Lin, Z. Q. *Macromolecules* **2011**, *44*, 7176–7183.
- Li, Z. C.; Ono, R. J.; Wu, Z. Q.; Bielawski, C. W. *Chem. Commun.* **2011**, *47*, 197–199.
- Kamps, A. C.; Fryd, M.; Park, S. *J. ACS Nano* **2012**, *6*, 2844–2852.
- Patel, S. N.; Javier, A. E.; Stone, G. M.; Mullin, S. A.; Balsara, N. P. *ACS Nano* **2012**, *6*, 1589–1600.
- Ge, J.; He, M.; Qiu, F.; Yang, Y. L. *Macromolecules* **2010**, *43*, 6422–6428.
- Wu, P. T.; Ren, G. Q.; Li, C. X.; Mezzenga, R.; Jenekhe, S. A. *Macromolecules* **2009**, *42*, 2317–2320.
- Yokoyama, A.; Miyakoshi, R.; Yokozawa, T. *Macromolecules* **2004**, *37*, 1169–1171.
- Muller, C.; Goffri, S.; Breiby, D. W.; Andreasen, J. W.; Chanzy, H. D.; Janssen, R. A. J.; Nielsen, M. M.; Radano, C. P.; Siringhaus, H.; Smith, P.; Stingelin-Stutzmann, N. *Adv. Funct. Mater.* **2007**, *17*, 2674–2679.
- Zhao, K.; Ding, Z. C.; Xue, L. J.; Han, Y. C. *Macromol. Rapid Commun.* **2010**, *31*, 532–538.
- Scharsich, C.; Lohwasser, R. H.; Sommer, M.; Asawapirom, U.; Scherf, U.; Thelakkat, M.; Neher, D.; Kohler, A. *J. Polym. Sci. Part B: Polym. Phys.* **2012**, *50*, 442–453.